THE ODD-PROTON EFFECTS ON THE POTENTIAL ENERGY SURFACES OF ODD MASS Tl, Au, Ir and Re ISOTOPES.

W. de Wieclawik*, I. Ragnarsson**, S.E. Larsson**, G. Leander**, Ch. Vieu*** and J.S. Dionisio***

* I.P.N. (Div. Phys. Nucl.) 91406 Campus Orsay, FRANCE

** Lund Institute of Technology (Dep. Math. Phys.) Lund 7, SWEDEN

*** C.S.N.S.M. (IN2P3) Lab. Salomon Rosenblum, 91406 Campus Orsay, FRANCE

Abstract

The total potential energy surfaces of thallium, gold, iridium and rhenium odd mass isotopes are calculated microscopically as functions of the quadrupole deformation, ε_2, when the odd protons occupy definite orbitals. The nuclear shapes and the static equilibrium deformations of these nuclei are deduced from the results of these calculations for the proton orbitals nearest to the Fermi level. The influence of the hexadecapole deformation, ε_4, on these results is investigated too. Finally, a few experimental data available for these odd mass nuclei are correlated to the corresponding theoretical results.

1. Introduction

The odd proton nuclei of the transition region between the rare-earth elements and the ^{208}Pb double closed shell (Tl, Au, Ir, Re) were extensively investigated experimentally during the last few years. Furthermore several theoretical descriptions of their properties were given assuming a single proton (hole, quasi-proton or proton hole cluster) coupled to vibrations or rotations of a spherical (or deformed) core [1-7]. However there is not yet available a systematic investigation of the odd proton effect on the static collective properties of these nuclei. Indeed, preliminary investigations were made in this direction earlier but they were restricted to a few odd proton nuclides near the single proton closed shells Z = 50 [8] and Z = 82 [9]. Furthermore in these calculations [8,9] only a few high and low spin proton orbitals were analysed in detail.

The purpose of the present investigation is to evaluate the total potential energy surfaces of thallium, gold, iridium and rhenium odd mass isotopes as functions of the quadrupole deformation parameter, ε_2, when the odd protons occupy definite orbitals in the modified oscillator model [10]. This analysis is restricted to the orbitals near to the Fermi level of each nuclide. Indeed they are expected to play a preponderant role on the description of these transitional nuclei. For each nuclide considered the total potential energy differences, V_{po}, between the oblate and prolate minima of the low lying orbitals as well as the quadrupole deformation parameters and possible shape transitions are discussed. Finally the influence of the hexadecapole deformation on the potential energy surfaces and other collective properties considered is also investigated.

2. Calculations

2.1. The model

The total potential energy surfaces of these odd proton nuclei are calculated microscopically with an extended version of the programme previously applied to even [11] and odd-mass [8] nuclei. In each case, the potential energy is a sum of two terms (the liquid drop and the shell correction energies) depending on two deformation (axial quadrupole ε_2 and hexadecapole ε_4) parameters. The main improvement relatively to the the old programme [11] is the possibility to put the odd proton on any given orbit.

2.2. The parametrization

In the present calculations, the adopted parametrization is nearly identical to the parameter set used for the neighbouring even-even nuclei [11]. The only differences are slight changes in the κ and μ parameters of the oscillator potential for the proton and neutron orbitals.

In most calculations reported here, it is assumed no hexadecapole deformation. However, in order to investigate the influence of the ε_4 deformation on these results, other calculations were made with $\varepsilon_4 \neq 0$.

2.3. Single proton and Fermi levels of Tl, Au, Ir and Re

A portion of the single proton level scheme corresponding to the transition region between the rare earth elements and the lead isotopes is represented in fig.1. In this diagram are also included the thallium, gold, iridium and rhenium Fermi levels determined with the same computing programme and parametrization. For clearness, only the Nilsson orbitals close to the Fermi levels of these nuclides are represented. Furthermore, the most important orbitals considered in the forthcoming discussion are full drawn.

2.4. Total potential energy

The projected total potential energy surfaces of a few odd mass Tl, Au, Ir and Re isotopes are represented in figs. 2-5 From their analysis, the total potential energy differences, V_{po}, between the oblate and prolate minimum, the absolute quadrupole deformation parameter $|\varepsilon_2|$ and the potential energy differences, E_{def}, between the lowest minimum and the corresponding spherical limit ($\varepsilon_2 = 0$) for the groundstate orbital are determined (fig.6-8). The same magnitudes are deduced from the potential energy curves corresponding to the orbitals belonging to the $1h_{9/2}$ and $1h_{11/2}$ subshells

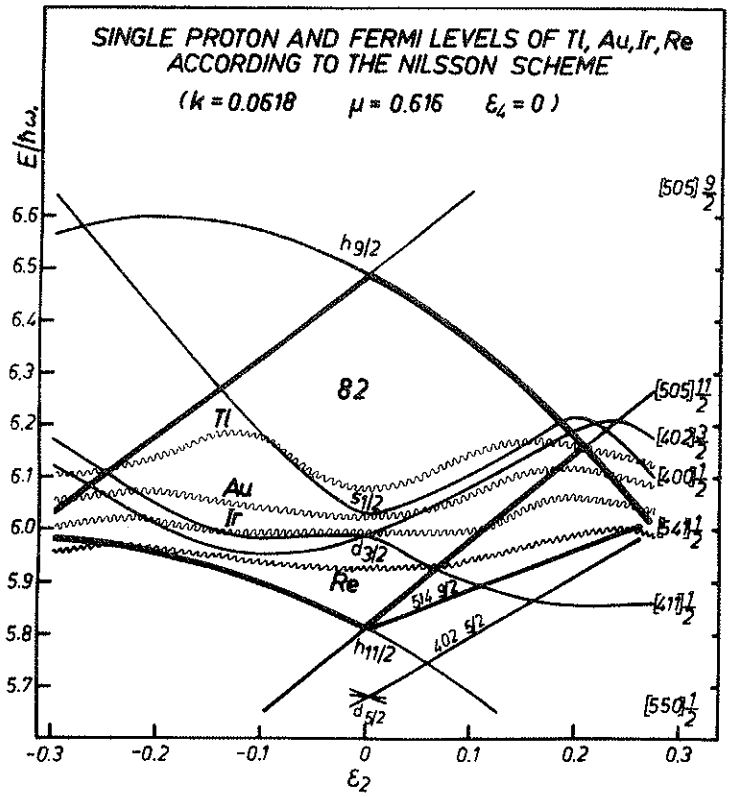

Fig.1 Partial single proton and Fermi levels of Tl, Au, Ir and Re isotopes. Only the Nilsson orbitals close to the Fermi levels of these nuclides are represented.

(figs. 9-13). To investigate their dependence on the neutron number, the experimental and theoretical results of given isotopes are presented and discussed simultaneously. Furthermore , for greater clearness, the positive and negative parity orbitals are considered separately. Finally, the analysis of the ε_4 influence is illustrated in the case of negative parity orbitals (figs. 15, 16).

3. Analysis of the results

3.1. Thallium isotopes

According to the position of the Thallium Fermi level, the $1/2^+[400]$, $3/2^+[402]$ and $1/2^+[411]$ orbitals should be the most relevant configurations for the description of the positive parity states. Similarly, the $9/2^-[505]$ (or $1/2^-[541]$), $11/2^-[505]$ (or $1/2^-[550]$) orbitals should be the preponderant configurations for the description of the negative parity states.

3.1.1. Positive parity orbitals

The ground state, $1/2^+$, of all odd mass Thallium isotopes is identified to the $1/2^+[400]$ single proton configuration. Indeed this configuration is the closest to the Fermi level for small quadrupole deformations $|\varepsilon_2| \lesssim 0.15$. The corresponding potential energy curves (fig.2) show two flat minima giving no clear indication of static quadrupole deformations. However, the V_{po} diagram (fig.6) predicts a small quadrupole oblate deformation for the light and medium Tl isotopes in their ground states. Indeed the calculated absolute quadrupole deformation parameter (fig.7) is small ($\varepsilon_2 \simeq 0.06$-$0.07$) and nearly independent of the neutron number. Nevertheless the small energy difference between the lowest oblate minimum $1/2^+[400]$ and the spherical limit, $3s_{1/2}$ of the potential energy curve (fig.8) compared to the zero point energy ($E_{zp} \simeq 1,09$ MeV) calculated for the heavier Tl isotopes [13] suggests a nuclear shape instability.

The first excited state with positive parity, $3/2^+$, in the odd mass Tl isotopes should have a large contribution of the orbital $3/2^+[402]$, according to the analysis of the single proton and Fermi levels (fig.1). The corresponding potential energy curves are slightly more asymmetric than those of the orbital $1/2^+[400]$. However this asymmetry is small and the corresponding minimum rather flat. Consequently the Tl isotopes in their ground and first excited states are expected to behave like soft vibrators.

3.1.2. Negative parity orbitals

All the potential energy curves corresponding to the high spin $9/2[505]$ orbitals of the $1h_{9/2}$ proton subshell (fig.2) have a minimum at a finite deformation on the oblate side ($\varepsilon_2 \lesssim -0.10$). This minimum is deeper than the corresponding one of the $1h_{9/2}$ low spin $1/2[541]$ orbital appearing at $\varepsilon_2 \gtrsim 0.08$. The same conclusion can be drawn from the analysis of the V_{po} diagram (fig.9). Indeed, Vpo is negative and nearly constant ($V_{po} \lesssim 0.50$ MeV) for all Tl isotopes. However, for the heavier thallium isotopes ($N \gtrsim 120$), the V_{po} curve decreases rapidly. The quadrupole deformation parameter has a similar behaviour. Moreover, the

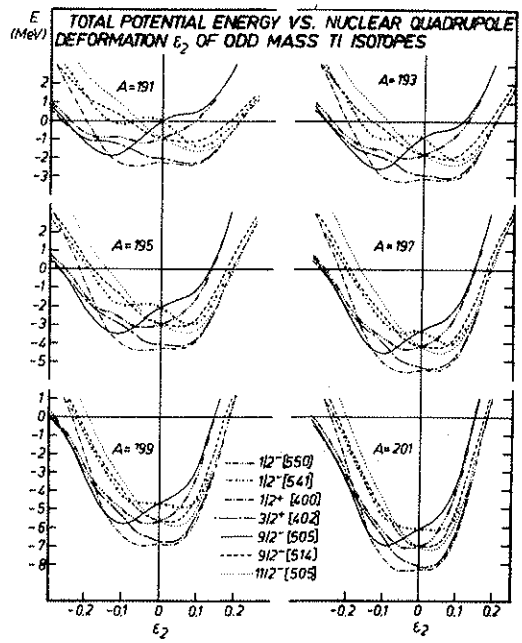

Fig.2 Total potential energy dependence on the nuclear quadrupole deformation, ε_2, of a few odd mass Tl isotopes in their lowest positive and negative parity orbitals.

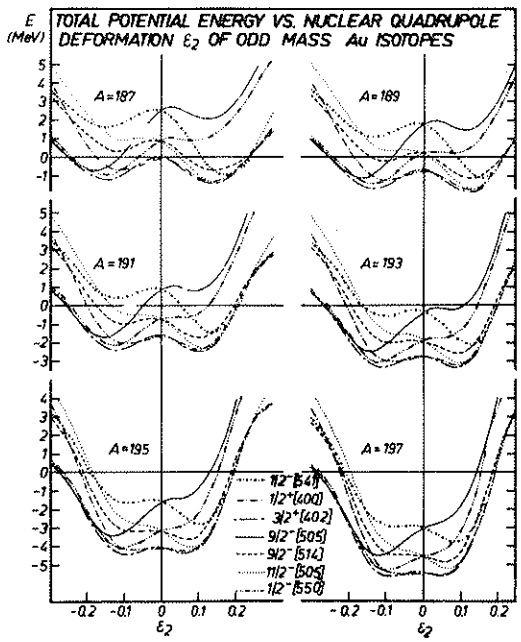

Fig.3 Total potential energy dependence on the nuclear quadrupole deformation, ε_2, of a few odd mass Au isotopes in their lowest positive and negative parity orbitals.

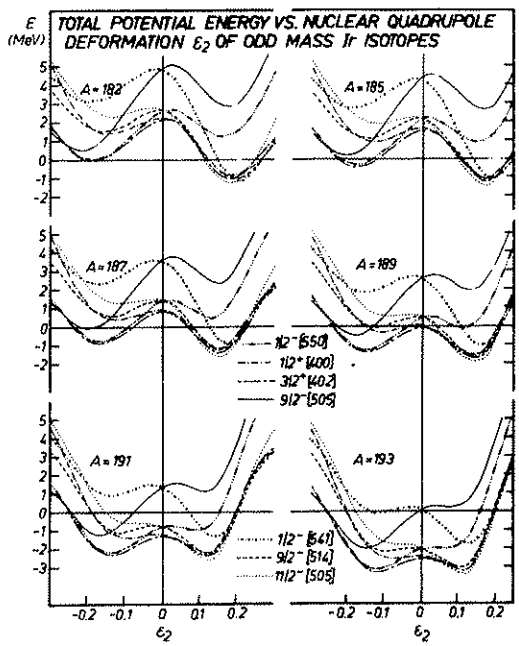

Fig.4 Total potential energy dependence on the nuclear quadrupole deformation, ε_2, of a few odd mass Ir isotopes in their lowest positive and negative parity orbitals.

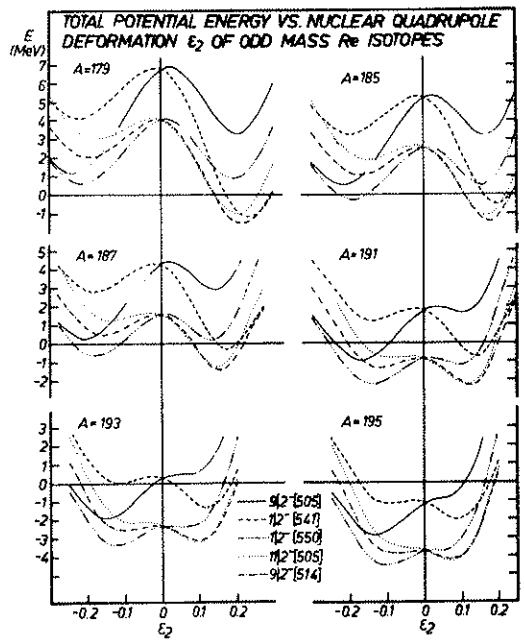

Fig.5 Total potential energy dependence on the nuclear quadrupole deformation, ε_2, of a few odd mass Re isotopes in their lowest negative parity orbitals.

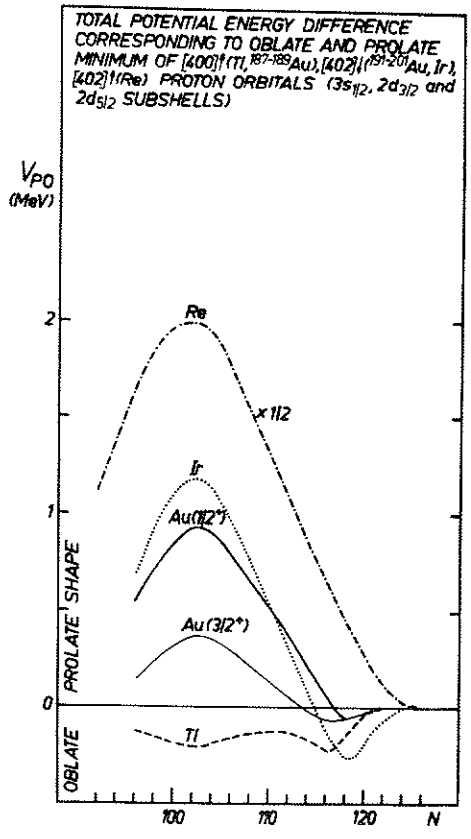

Fig.6 Total potential energy difference between the oblate and the prolate minima of Tl, Au, Ir and Re in the groundstate proton orbital

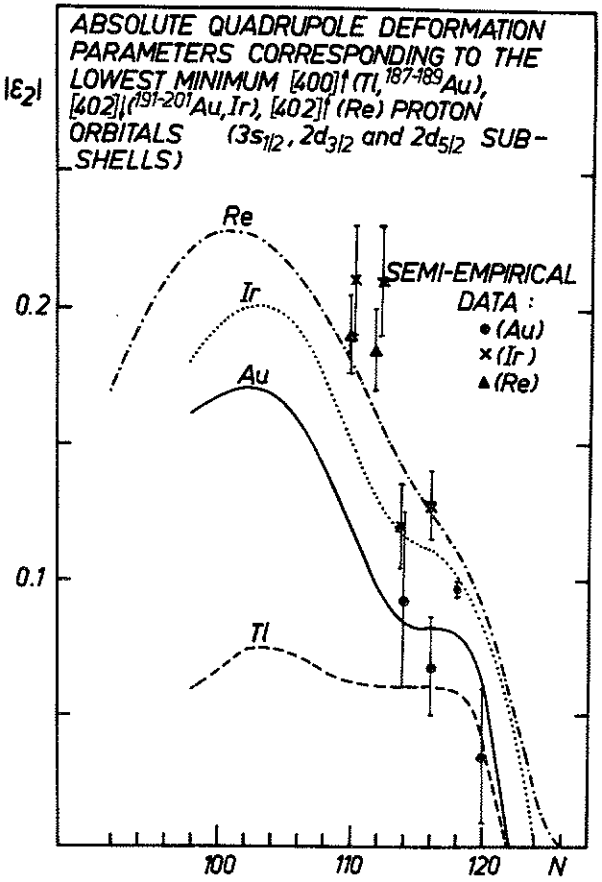

Fig.7 Absolute quadrupole deformation parameters corresponding to Tl, Au, Ir and Re groundstate orbitals. For the semi empirical data see text.

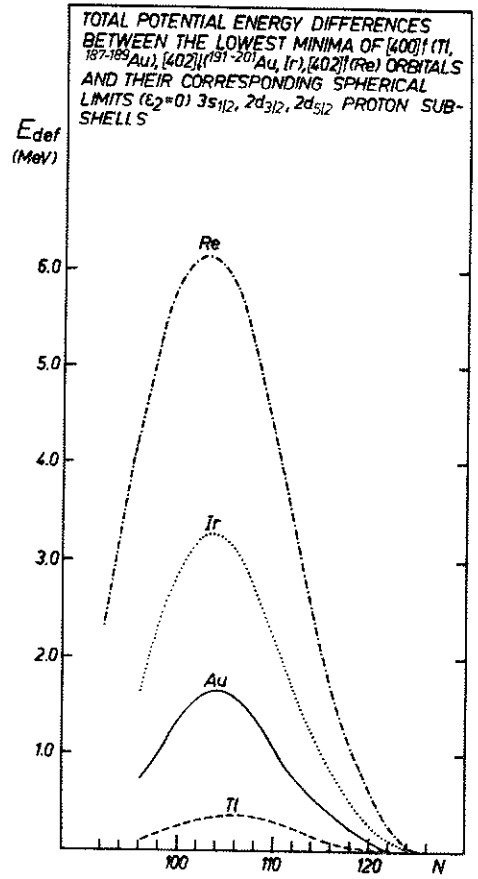

Fig.8 Total potential energy differences between the lowest minima of Tl, Au, Ir and Re in the groundstate orbitals and the corresponding spherical limit.

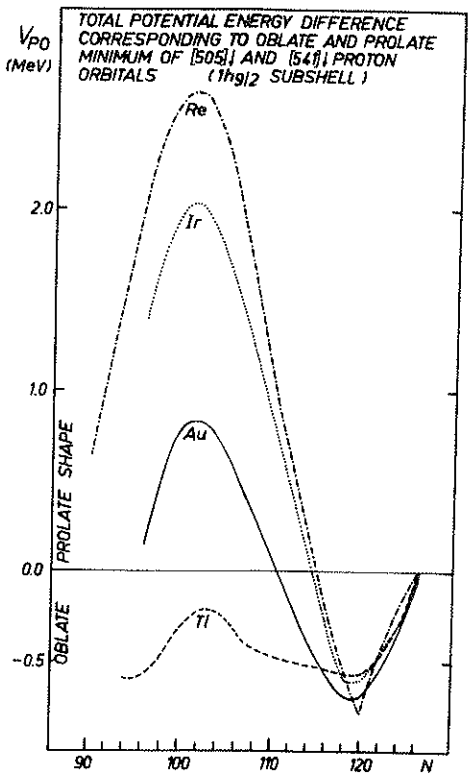

Fig.9 Total potential-energy difference between the oblate and prolate minima of the 9/2[505] and 1/2[541] proton orbitals.

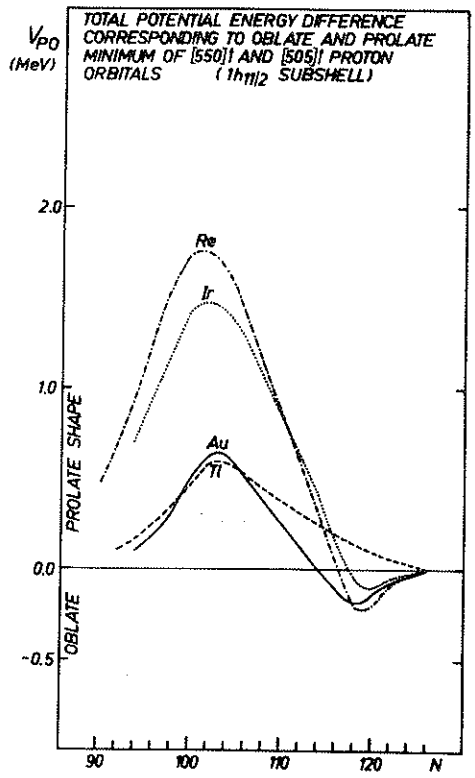

Fig.10 Total potential energy difference between the oblate and prolate minima of the 1/2[550] and 11/2[505] proton orbitals.

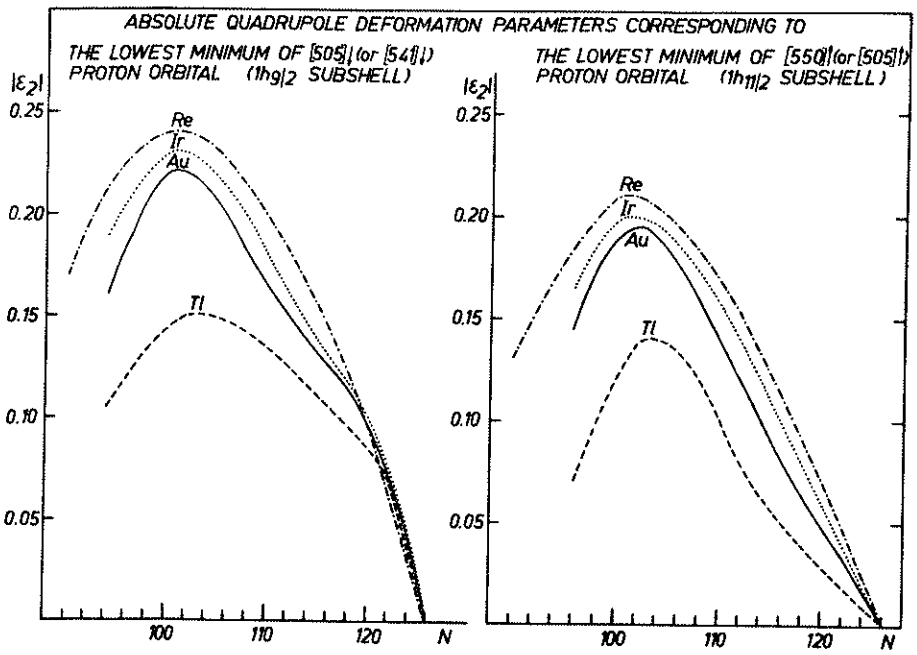

Fig.11a Absolute quadrupole deformation corresponding to the lowest minimum of 9/2[505] or 1/2[541] proton orbital.

Fig. 11b Absolute quadrupole deformation corresponding to the lowest minimum of 1/2[550] or 11/2[505] proton orbital.

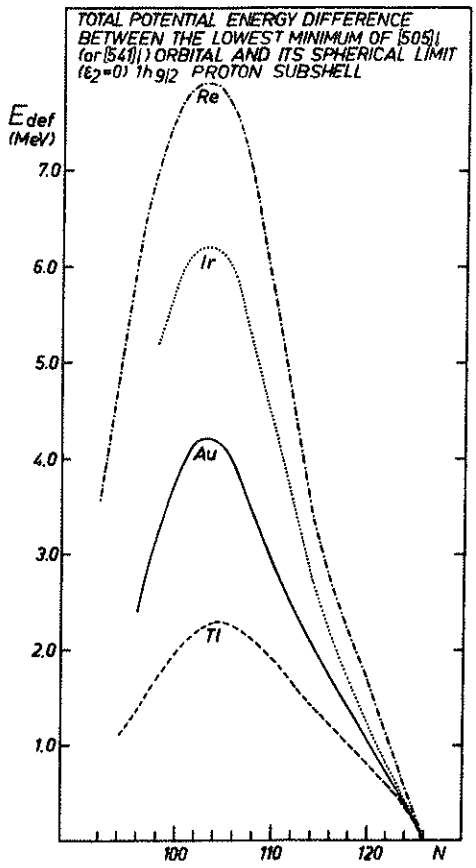

Fig.12 Total potential energy difference between the lowest minimum of 9/2[505] (or 1/2 [541]) orbital and its spherical limit (ε_2=0) $1h_{9/2}$ proton subshell.

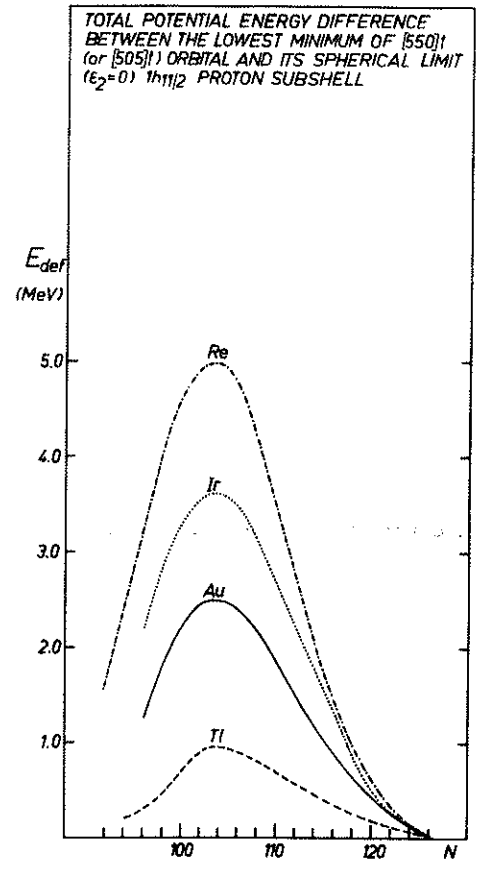

Fig.13 Total potential energy difference between the lowest minimum of 1/2[550] (or 11/2 [505]) orbital and its spherical limit (ε_2=0) $1h_{11/2}$ proton subshell.

broad and small E_{def} curve ($E_{def} \leqslant 1$ MeV for $N \geqslant 120$ fig.12) suggests a spherical shape for the heavier Tl isotopes which should behave like spherical vibrators.

A similar analysis of the 1/2[550] and 11/2[505] potential energy curves (fig.2) and the V_{po} diagrams indicate prolate equilibrium deformations for all the Tl isotopes. However, for $N \geqslant 114$, the V_{po} differences and the ε_2 deformations are small ($V_{po} \leqslant 0.20$ MeV fig.10; $\varepsilon_2 \leqslant 0.06$ fig.7). Finally, no significant departure from spherical shape is predicted for the heavier isotopes from the E_{def} values ($E_{def} \leqslant 0.5$ MeV for $N > 114$ fig.13) on account of the neglected zero point energy contribution.

3.2. Gold isotopes

According to fig.1, the 3/2[402] (or 1/2[411]), 1/2[400], 9/2[505] (or 1/2[541]), and 11/2[505] (or 1/2[550]) orbitals are the preponderant configurations for the description of the groundstate and the low and medium excited levels in gold.

3.2.1 Positive parity orbitals

The potential energy curves (fig.3) and the V_{po} diagrams (fig.6) corresponding to the 3/2[402] (or 1/2[411]) and 1/2[400] orbitals suggest prolate deformations for the light gold in their $1/2^+$ or $3/2^+$ groundstate. The greatest deformation is attained in the 1/2[400] orbital where $0.10 \leqslant \varepsilon_2 \leqslant 0.17$. Moreover, the V_{po}, $|\varepsilon_2|$ and E_{def} diagrams give indications for a possible shape transition for the $3/2^+$ groundstate of the heavier gold isotopes (fig.6-8). For these isotopes, there is a satisfactory agreement between the static theoretical ε_2 and the dynamic semi-empirical quadrupole deformations deduced from the relation:

$$\varepsilon_2 = \sqrt{45/16\pi}\ \beta - 15/16\pi\ \beta^2$$

where β is determined from the experimental B(E2) values of the $5/2^+_1 \rightarrow 3/2^+_1$ transitions as described in ref.15.

3.2.2 Negative parity orbitals

All the gold potential energy curves of the 9/2[505] and 1/2[541] orbitals have a minimum on the oblate (prolate) side at $\varepsilon_2 \approx -0.10$ (+0.10) like those of the Tl isotopes (fig.3). The nearly symmetric V_{po} diagrams of these orbitals (fig.9) predict prolate shapes for the light gold isotopes and oblate shapes for the heavier ones ($A \geqslant 189$). Consequently, a well defined shape transition is expected at N = 110 (or near by that neutron number) on account of the contribution of the zero point energy . Finally, the absolute quadrupole deforma-

tion $|\varepsilon_2|$ and the potential energy differences, E_{def}, corresponding to these $1h_{9/2}$ orbitals are considerably higher in the gold isotopes than in the thallium ones (figs.11a and 12).

A similar analysis of the potential energy curves of the 11/2[505] and 1/2[550] orbitals shows smaller asymmetry than in the $1h_{9/2}$ lowest orbitals (fig.3). Furthermore, the V_{po} diagrams predict prolate deformations for the light gold isotopes (fig.10). A shape transition may occur for the heavier ones (A ⩾ 114) but it is less clear than for the $1h_{9/2}$ lowest orbitals due to the smallness of the oblate V_{po} minimum ($V_{po} \leqslant 0.20$ MeV). Similarly, the corresponding $|\varepsilon_2|$ and E_{def} curves (fig.11b ,13) do not give any clear indication of a permanent oblate deformation.

3.3. Iridium isotopes

The Fermi levels of the iridium and gold isotopes are close and parallel for $|\varepsilon_2| \leqslant 0.3$ (fig.1). Consequently, one expects the same preponderant effects of the same odd proton configurations in both elements apart the different influence of three and five proton hole clusters in the lead shell.

3.3.1. Positive parity orbitals

The potential energy curves corresponding to the positive parity configurations 1/2[400]and 3/2[402] of the heavier iridium isotopes (^{191,193}Ir) have a similar shape (fig.4) to the curves of the light gold isotopes (^{187,189}Au). Furthermore, the potential energy differences V_{po} predict prolate quadrupole deformations for the positive parity states of the light iridium isotopes and a possible shape transition at N = 114 for the $3/2^+$ groundstate (fig.6).

A better agreement between the semi-empirical and the static ε_2 values is obtained for the heavier (N ⩾ 114) than for the lighter iridium isotopes (fig.7). However, the experimental B(E2) results [16] are too much scattered in order to derive any definite conclusion from this comparison.

Finally, the total potential energy difference , E_{def}, between the lowest minimum of the Ir groundstate orbital and the corresponding $2d_{3/2}$ spherical limit is larger than in Tl and Au isotopes (fig.8). Consequently, these calculations predict a considerable permanent prolate deformation for the Ir isotopes in their ground states.

3.3.2. Negative parity orbitals

The projected total potential energy surfaces corresponding to the lowest orbitals of the $1h_{9/2}$ subshell in all the Ir isotopes (fig. 4) have deep minima on the oblate or prolate sides (for $0.12 \leqslant |\varepsilon_2| \leqslant 0.17$). Furthermore, similar shape transitions previously observed for these orbitals in gold, occur also in iridium (fig. 9). However, the V_{po} iridium curve is more asymmetric than the gold one. Such fact is stressed by the E_{def} curve which shows a larger energy difference for the prolate ($E_{def} \simeq 6$ MeV for N=104) than for oblate ($E_{def} \simeq 1.0$ MeV for N=120) lowest $1h_{9/2}$ iridium orbitals (fig. 12). Finally, the absolute quadrupole deformations, $|\varepsilon_2|$, are nearly identical in Ir and Au isotons (fig. 11a).

The same analysis of the potential energy curves corresponding to the highest $1h_{11/2}$ iridium orbitals (fig. 10) leads to similar conclusions previously obtained for the gold isotopes (sect. 3.2.2). In particular, the prolate part of the V_{po} curve is steeper in iridium than in gold. On the contrary, no clear evidence exists for permanent oblate shapes in the 1/2 [550] orbital. Furthermore, the $|\varepsilon_2|$ deformations of the isotons of both elements are nearly identical (fig. 12b). However, the maximum value of Edef in the Ir isotopes is nearly proportional to the corresponding values of Tl and Au isotons (fig. 13).

3.4. Rhenium isotopes

The ground state and low lying excited states of the odd mass Re isotopes are based essentially on 5/2[402] and 9/2[514] proton orbitals due to their lower Fermi level and greater quadrupole prolate deformation.

3.4.1. Positive parity orbitals

The total potential energy dependence on the nuclear quadrupole deformation, ε_2, of a few odd mass rhenium isotopes in their groundstate is represented in fig. 14.

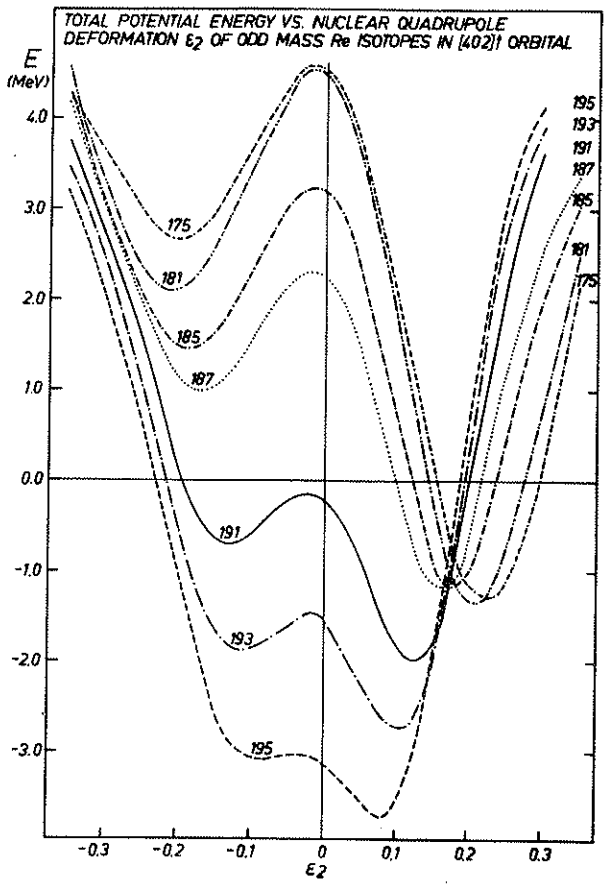

Fig.14 Total potential energy dependance on the quadrupole deformation, ε_2, of a few odd mass Re isotopes in the 5/2[402] orbital.

These curves are slightly asymmetric in the heavy isotopes (^{195}Re) but strongly asymmetric in the light ones (^{175}Re). Consequently the prolate shapes are favoured in the latter nuclides, as shown in the V_{po}, $|\varepsilon_2|$ and E_{def} diagrams (figs. 6-8). The semi-empirical deformation parameters represented in fig. 7 were deduced from data taken in ref. 14 with the errors approximately estimated.

3.4.2. Negative parity orbitals

The total potential energy dependence on the nuclear quadrupole deformation of a few odd mass rhenium isotopes in their lowest $1h_{9/2}$ and highest $1h_{11/2}$ proton orbitals is represented in fig. 5. Following the general trend of this systematic study, the V_{po}, $|\varepsilon_2|$ and E_{def} diagrams (figs.9-13) corresponding to the same orbitals were deduced from the analysis of the potential energy curves. However, there is not yet any experimental evidence for rhenium excited states built on the prolate (oblate) 1/2[541] (9/2[505]) or 11/2[505] (1/2[550]) orbitals. Indeed, the low and medium excited negative parity levels of the odd mass Re isotopes are built on 9/2[514] proton orbital. For that reason, this orbital was also included in the total potential energy curves of Tl, Au and Ir isotopes (figs.2-4).

3.5. Influence of the ε_4 deformation

The V_{po} diagram given in figure 15 is relative to the lowest $1h_{9/2}$ and the highest $1h_{11/2}$ orbitals. Moreover, the $\varepsilon_4(\varepsilon_2)$ dependence is represented graphically in the inset of the same figure. From the comparison between the figures 9, 10 and 15, one sees a relatively small increase of the V_{po} values of the different isotopes. The biggest changes are for the $1h_{9/2}$ lowest orbitals of thallium. Similar differences are not observed for the other elements. In particular, the shape transitions are independent of these small ε_4 deformations.

The E_{def} diagrams represented in figure 16 correspond to the same $1h_{9/2}$ and $1h_{11/2}$ orbitals and $\varepsilon_4(\varepsilon_2)$ dependence previously quoted. The comparison between this figure

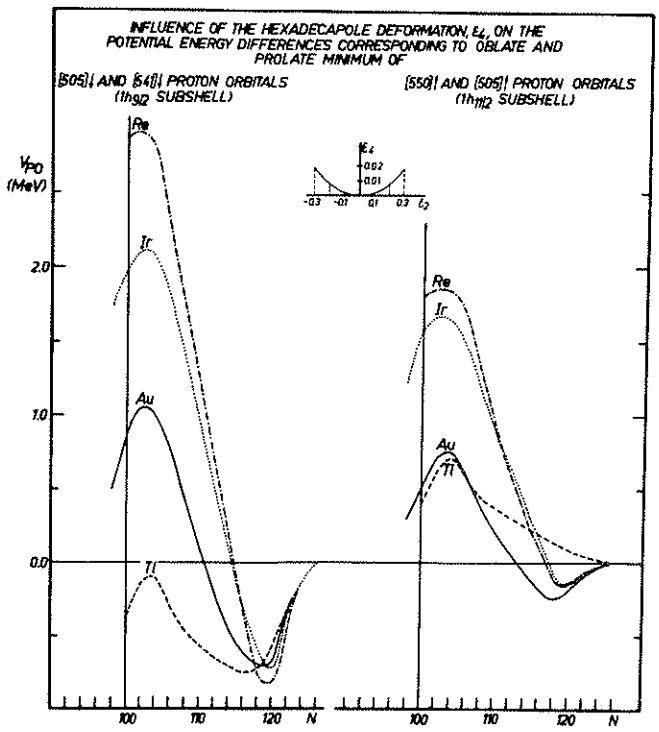

Fig.15 Potential energy differences, V_{po}, corresponding to the same orbitals as considered in figures 9 and 10

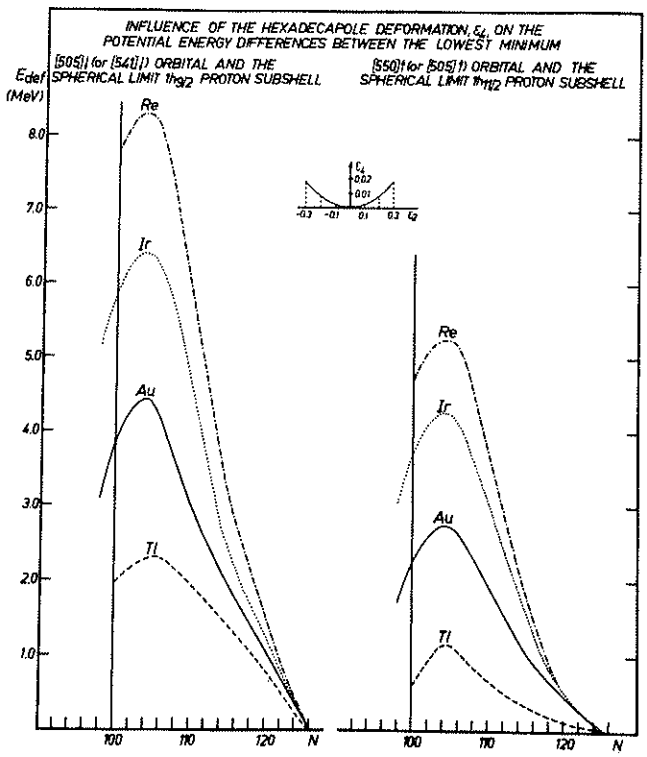

Fig.16 Potential energy differences, E_{def}, corresponding to the same proton orbitals as considered in figures 12 and 13.

and the corresponding ones where ε_4 deformation was neglected (figs.12,13) reveals a small influence of hexadecapole deformation for the elements considered.

4. Conclusions

This systematic investigation of the odd proton effects in Tl, Au, Ir and Re isotopes leads to the following conclusions:

- The positive parity states based on the low spin 1/2[400], 3/2[402] or 5/2[402] proton configurations correspond to small oblate (Tl) or medium prolate (Au, Ir, Re) quadrupole deformations.
- The negative parity states, built on proton hole states in the highest Nilsson orbitals of the $1h_{11/2}$ subshell, are connected with relatively stable prolate quadrupole deformations.
- The negative parity states, arising from proton particle states in the lowest Nilsson orbitals of the $1h_{9/2}$ subshell, correspond to prolate ε_2 defor-

mations in Au, Ir and Re isotopes. Such sharp transitions of the shape are not observed in Tl isotopes where the lowest $1h_{9/2}$ particle orbitals have smaller influence ($\langle\varepsilon_2\rangle \simeq -0.10$) for all these isotopes.

References

1. *Proceedings of the International Conference on Nuclear Structure and Spectroscopy, Nuclear models in theory and experiment*, ed. H.P. Blok and A.E.L. Dieperink, (Amsterdam 1974) vols. I and II.
2. *Proceedings of the Topical Conference on Problems of Vibrational Nuclei, Zagreb 1974*, G. Alaga, V. Paar and L. Sips, North Holland Publ. Comp. Amsterdam 1975.
   Proceedings of the Topical Conference on Problems of Vibrational Nuclei, Zagreb 1974, ed. G. Alaga, V. Lopac, V. Paar and L. Sips, in Fizika, vol.7 Supp.2 (1975).
3. *Proceedings of the XXI National Conference on Nuclear Spectroscopy and Nuclear Structure, Leningrad 1975*, in Izv. Akad. Nauk. SSSR 40 (1976) n°1.
4. *Comptes Rendus du Colloque sur la surface des Noyaux, Dijon 1975*, J. de Phys. Colloque C5 (1975) 36.
5. *Proceedings of the International Symposium on Nuclear Structure, Coexistence of single particle and collective type excitation, Balatonfured 1975*, ed. F. Lovas and G. Palla, vols. I, II
6. *Proceedings of the International Symposium on highly excited states in nuclei, Jülich 1974*, ed. A. Faessler, C. Mayer-Böriche and P. Turek, Jülich Conf. 16 vol.I
7. *Proceedings of the XXVI National Conference on Nuclear Spectroscopy and Nuclear Structure, Baku 1976*, to be published in Izv. Akad. Nauk. SSSR.
8. *I. Ragnarsson and S.G. Nilsson, in Les noyaux de transition, Rapport sur l'état actuel des études expérimentales et théoriques*, ed. R. Foucher, N. Perrin and M. Veneroni, Orsay 1971, 112
9. J. Leyttenhove, K. Heyde, H.Vincz and M. Warroquier, Nucl. Phys. A241 (1975) 135.
10. S.G. Nilsson, C.F. Tsang, A. Sobiczewski, Z. Szymanski, S. Wycech, C. Gustafson, I.L. Lamm, P. Möller and B. Nilsson, Nucl. Phys. A131 (1969) 1.
11. I. Ragnarsson, A. Sobczewski, R.K. Sheline, S.E. Larsson and B. Nerlo-Pomorska, Nucl. Phys. A233 (1974) 329.
12. H. Ohlsson, *Courbes et surfaces d'énergie potentielle collective d'après le programme de S:G. Nilsson*, Internal Report Ph. Nucl. 7208, IPN Orsay 1971.
13. K. Kumar and M. Baranger, Nucl. Phys. A122 (1968) 273.
14. K.E.G. Löbner, M. Vetter and V. Honig, Nuclear Data Tables A7 (1970) 495.
15. Ch. Vieu, Thesis Orsay 1974.
16. C. Sebille-Schuck, M. Finger, R. Foucher, J.P. Husson, J. Jastrzebski, V. Berg, S.G. Malmskog, G. Astner, B.R. Erdal, P. Patzelt and P. Siffert Nucl. Phys. A212 (1973) 45.